HHS Public Access

Author manuscript

Math Biosci Eng. Author manuscript; available in PMC 2015 December 10.

Published in final edited form as:

Math Biosci Eng. 2014 June ; 11(3): 621–639.

MODELING THE ENDOCRINE CONTROL OF VITELLOGENIN PRODUCTION IN FEMALE RAINBOW TROUT

Kaitlin Sundling,
Biophysics Program and Medical Scientist Training Program, University of Wisconsin, Madison, WI 53706, USA

Gheorghe Craciun,
Department of Mathematics and Department of Biomolecular Chemistry, University of Wisconsin, Madison, WI 53706, USA

Irvin Schultz,
Battelle Pacific Northwest National Laboratory, Marine Sciences Laboratory, Sequim, WA 98382, USA

Sharon Hook,
Battelle Pacific Northwest National Laboratory, Marine Sciences Laboratory, Sequim, WA 98382, USA

James Nagler,
Department of Biological Sciences and Center for Reproductive Biology, University of Idaho, Moscow, ID 83844, USA

Tim Cavileer,
Department of Biological Sciences and Center for Reproductive Biology, University of Idaho, Moscow, ID 83844, USA

Joseph Verducci,
Department of Statistics, Ohio State University, Columbus, OH 43210, USA

Yushi Liu,
Department of Statistics, Ohio State University, Columbus, OH 43210, USA

Jonghan Kim, and
Department of Pharmaceutical Sciences, Northeastern University, Boston, MA 02115, USA

William Hayton
Division of Pharmaceutics, Ohio State University, Columbus, OH 43210, USA

Kaitlin Sundling: ksundling@wisc.edu; Gheorghe Craciun: craciun@math.wisc.edu; Irvin Schultz: irv.schultz@pnnl.gov; Sharon Hook: sharon.hook@csiro.au; James Nagler: jamesn@uidaho.edu; Tim Cavileer: tcavi@uidaho.edu; Joseph Verducci: jsv@stat.osu.edu; Yushi Liu: liuyushi@gmail.com; Jonghan Kim: j.kim@neu.edu; William Hayton: hayton.1@osu.edu

Abstract

2010 *Mathematics Subject Classification*. Primary: 92C45, 92B05; Secondary: 37N25, 92C30, 92C42.

The rainbow trout endocrine system is sensitive to changes in annual day length, which is likely the principal environmental cue controlling its reproductive cycle. This study focuses on the endocrine regulation of vitellogenin (Vg) protein synthesis, which is the major egg yolk precursor in this fish species. We present a model of Vg production in female rainbow trout which incorporates a biological pathway beginning with sex steroid estradiol-17β levels in the plasma and concluding with Vg secretion by the liver and sequestration in the oocytes. Numerical simulation results based on this model are compared with experimental data for estrogen receptor mRNA, Vg mRNA, and Vg in the plasma from female rainbow trout over a normal annual reproductive cycle. We also analyze the response of the model to parameter changes. The model is subsequently tested against experimental data from female trout under a compressed photoperiod regime. Comparison of numerical and experimental results suggests the possibility of a time-dependent change in oocyte Vg uptake rate. This model is part of a larger effort that is developing a mathematical description of the endocrine control of reproduction in female rainbow trout. We anticipate that these mathematical and computational models will play an important role in future regulatory toxicity assessments and in the prediction of ecological risk.

Key words and phrases

Endocrine control; vitellogenin; pharmacokinetic/pharmacodynamic model

1. Introduction

In order to reproduce in their natural environment, fish must respond appropriately to environmental signals such as temperature, food availability and changing light conditions. These environmental cues are integrated at the level of the brain and result in endocrine changes that regulate gonad development and eventually gamete production and release. This study seeks to model the endocrine control of an important biological pathway that is critical for ovary development in female rainbow trout *Oncorhynchus mykiss*, an iteroparous, egglaying fish with a group synchronous annual reproductive cycle. Rainbow trout, like other salmonid fishes, are particularly sensitive to photoperiod and changing annual day length is the principal environmental cue controlling reproduction [9, 10, 4]. Changes in photoperiod, particularly decreasing photoperiod, have been shown to accelerate rainbow trout sexual maturation as evidenced by increasing gonad size [2], and plasma follicle stimulating hormone and sex steroid concentrations [2, 8]. Although the precise endocrine pathway is not known, changing light levels do affect gonadotropin-releasing hormone production in the brain, which in turn stimulates pituitary release of gonadotropins which have downstream effects on the ovaries [40]. This study focuses on the endocrine regulation of vitellogenin (Vg) protein synthesis, which is the major egg yolk precursor in this species. Vg is produced in the liver upon stimulation by the sex steroid estradiol-17β (E2), which is primarily synthesized in the ovaries. Proper regulation of Vg production is essential for successful egg development [35].

In a previous study, we developed an initial pharmacokinetic/pharmacodynamic (PK/PD) model of the salmon brain-pituitary-ovarian axis, which described the synthesis and biological activity of several essential reproductive hormones produced by these tissues

including E2 [16]. The model was based on previously published data obtained from female Coho salmon and did not include a description of vitellogenesis. In a separate unpublished effort, Kim [15] developed a PK/PD model of Vg production in male rainbow trout after prolonged waterborne exposure to a potent synthetic estrogen, ethinylestradiol. This latter model included a description of E2 binding to a hepatic receptor that stimulated Vg synthesis. The model also included a description of Vg clearance from plasma based on previous experimental studies in male trout [31]. The model in [15] provided simulations that adequately matched the experimentally observed plasma profile of Vg [32] in the ethinylestradiol exposed male trout.

Our prior published and unpublished modeling efforts have led us to develop a more comprehensive PK/PD model combining a brain-pituitary-ovarian module with a mathematical model of vitellogenesis in female rainbow trout. In the present study, we adapt the model in [15] to female rainbow trout by beginning with E2 levels in the plasma and concluding with Vg secretion by the liver and sequestration in the oocytes. Estradiol in the plasma is taken up by the liver, where it binds to an intracellular estrogen receptor [25]. In rainbow trout as with other vertebrates, there are two estrogen receptor subtypes denoted α and β [24]. In many fishes including trout, gene duplication has caused multiple isoforms of each subtype producing a total of four estrogen receptor isoforms (α_1, α_2, β_1 and β_2) [24, 18]. Although there is emerging data for some fishes that the estrogen receptor β isoforms may be involved in modulating Vg synthesis [26, 19], the experimental evidence for rainbow trout suggests the E2 induced synthesis of Vg is predominately regulated by estrogen receptor α_1 [3]. Thus, in our model we have assumed the E2-α_1 receptor complex activates transcription of both estrogen receptor mRNA and Vg mRNA. Translation produces Vg protein in the liver, which is secreted into the plasma and taken up by the ovary. We have modified the model in [15] by replacing some Michaelis-Menten terms by mass-action terms and by removing some inhibitory terms, in addition to adapting the model to female rainbow trout by parameter changes. The model was first fitted to experimental data from female rainbow trout over a normal 365 day photoperiod. The model was subsequently evaluated against experimental data from female trout reared under an artificially compressed 217 day photoperiod, which was intended to accelerate the reproductive cycle.

2. Description of model and methods

2.1. Biological description

Our model for Vg production in female trout incorporates eight variables distributed between three tissue compartments: ovary, plasma and liver (see the model diagram in Figure 2.1, model equations (2.1), and parameter definitions in Table 1). The initial driving force behind Vg production in our model is E2 in the plasma. We assume there is free and rapid diffusion of unbound E2 between the plasma and liver compartments so the concentrations can be taken to be equal [29, 33]. E2 then binds to a hepatic nuclear estrogen receptor R, produced by transcription of the estrogen receptor mRNA denoted mR. The rate constant $k_{s,r}$ describes the production of R by translation of mR (without corresponding loss of mR). E2 and R in association form the estrogen receptor complex ER, which is assumed

to be activated rapidly on E2 binding. The rate constants k_{on} and k_{off} describe the association and dissociation, respectively, of E2 and R. The ER complex acts as a transcription factor that activates the transcription of mR, with rate constant S_{mr} in an auto-regulatory positive feedback loop [11, 3]. Transcription is activated by the ER complex binding to estrogen response elements in the promoter region of the gene [11]. For simplicity, we assume that activation happens on a one-to-one ratio, as suggested by experimental data showing that a given dose of E2 yields similar increases in ER and Vg mRNA levels [11]. The ER complex also activates the transcription of Vg messenger RNA, mVg, with rate constant S_{mvg}. mVg is then translated via a transcription rate $k_{s,vg}$ and an amplification factor γ to generate Vg protein in the liver (Vg_L). The amplification factor is a power that increases the contribution of mRNA concentration because one mRNA molecule can be translated many times [14]. We have also assumed the degradation rates of R, mR and mVg ($k_{e,r}$, $k_{e,mr}$ and $k_{e,mvg}$ respectively) are unchanging during the reproductive cycle. Once formed, the intracellular Vg protein is subsequently secreted into the plasma with rate constant k_{sec}. Vg in the main plasma compartment is denoted as Vg_1. Vg_1 is then taken up by the ovary, Vg_O, and also distributes from the plasma to the body tissues or peripheral compartment (Vg_2) analogous to that described in [31].

$$\frac{dmR}{dt}=k_{s,mr}(1+S_{mr}\cdot ER)-k_{e,mr}\cdot mR \quad (2.1)$$

$$\frac{dR}{dt}=k_{s,r}\cdot mR-k_{e,r}\cdot R-k_{on}\cdot E2\cdot R+k_{off}\cdot ER \quad (2.2)$$

$$\frac{dER}{dt}=k_{on}\cdot E2\cdot R-(k_{off}+k_{deg})ER \quad (2.3)$$

$$\frac{dmVg}{dt}=k_{s,mvg}(1+S_{mvg}\cdot ER)-k_{e,mvg}\cdot mVg \quad (2.4)$$

$$\frac{dVg_L}{dt}=k_{s,vg}\left(\frac{mVg}{k_{mvg}}\right)^{\gamma}-k_{sec}\cdot Vg_L \quad (2.5)$$

$$\frac{dVg_1}{dt}=\frac{k_{sec}\cdot Vg_L\cdot V_H+CL_{12vg}\cdot Vg_2-(CL_{12vg}+CL_{1Ovg}+CL_{vg})Vg_1}{V_{1vg}} \quad (2.6)$$

$$\frac{dVg_2}{dt}=\frac{CL_{12vg}\cdot Vg_1-CL_{12vg}\cdot Vg_2}{V_{2vg}} \quad (2.7)$$

$$\frac{dVg_O}{dt}=CL_{1Ovg}\cdot Vg_1 \quad (2.8)$$

2.2. Experimental data

All rainbow trout were maintained according to guidelines established by the Institutional Animal Care and Use Committees (IACUC) of Battelle Pacific Northwest National Laboratory. Three-year old female rainbow trout were obtained from a commercial trout hatchery (Troutlodge, Inc., Sumner, WA). Two different groups of trout were used with one group spawned (eggs manually removed) on November 12, 2006 and the other group spawned on April 30, 2007. For both groups, spawning occurred at the hatchery and was the first spawning event for all trout. Thus, all trout were entering their second reproductive cycle at initiation of the study. The day after spawning, the trout were transferred to the Battelle Marine Sciences Laboratory (Sequim, WA) and housed in groups of 70 fish in circular fiberglass tanks (1400 L volume). Trout spawned on April 30, 2007 were held in an isolation room that allowed independent control of photoperiod. The lighting system and light intensity above each holding tank was identical. All tanks were maintained with a single pass flow-through freshwater system with water in-flow rates set to 20–25 L/min. The source water was from Battelle's artesian well (well depth = 134 m), and was pre-aerated before reaching holding tanks. Water quality parameters were routinely measured in both holding tanks with water temperature averaging 11.8°C (range: 11.0–12.8°C over the course of the study), dissolved oxygen > 9mg/l and pH 7.9 (range: pH 7.8–8.1 during the study). Throughout the study, all trout were fed a soft moist pelleted feed (6 mm in size) obtained from Bio-Oregon Inc, Longview, WA. The trout were fed three times a week at a ration level designed to maintain a constant body mass (approximately 0.5% body mass).

Initially, both groups of trout were maintained under lighting that simulates the natural photoperiod (NP) according to the latitude for Sequim WA, USA (48.079 N). The day after arrival at the Battelle Laboratory, the trout spawned on April 30, 2007 were reared under an artificial photoperiod that compressed the annual 365 day cycle to 217 days by incrementally adjusting the day length, in a proportionate manner, each day of the cycle.

During the normal and compressed photoperiod cycles, three trout were periodically removed at 17 different time points and anesthetized in an oxygenated solution of MS-222 (75 mg/L). After recording the body mass, blood was collected from the caudal vein using a heparinized syringe and 18 G needle. The plasma obtained by centrifugation (3000 g × 10 min) was flash frozen in liquid N2 and later stored at −80°C. After blood collection, trout were euthanized by decapitation and the whole pituitary and small portions of the liver and ovary were excised and immediately placed in RNAlaterTM solution (Ambion, Austin, TX), gradually chilled to 4°C overnight, and then frozen the next morning at −80°C for storage. Other small pieces of ovary were fixed in 10% formalin and eventually stored in 70% ethanol for histology. The total mass of the ovary and liver was recorded to the nearest 1/100g. The mean body weights (± SD) of the trout in the NP and SP groups were: 2021 ± 354 and 1887 ± 381 g respectively. Plasma samples were extracted twice with diethyl ether and the solvent extract analyzed by radioimmunoassay for estradiol-17β using a commercially available kit (Coat-A-Count Estradiol, Diagnostic Products, Los Angeles, CA) at the Center for Reproductive Biology Assay Core Laboratory (Department of Animal Sciences, Washington State University, Pullman, WA). Freshly thawed plasma samples

were analyzed for vitellogenin using a rainbow trout vitellogenin ELISA kit (Biosense, Cayman Chemical, Ann Arbor, MI).

2.3. Modeling methods

The numerical simulations were performed using the MATLAB function ode15s. Some parameters ($k_{s,mr}$, $k_{e,mr}$, S_{mr}, $k_{s,r}$, $k_{s,mvg}$, S_{mvg}, $k_{s,vg}$ and k_{sec}) were obtained by fitting the results of numerical simulations to experimental data. Other parameter values in Table 1 are derived from [15]. The E2 levels used for input are based on the experimentally measured values (Figure 2.2). The experimental data for E2 were smoothed using the MATLAB function csaps. The function csaps implements a cubic smoothing spline algorithm that produces a piecewise polynomial approximation of the data, given a weight vector and a smoothing parameter. In all our computations the data is weighted by 1/SD where SD is the standard deviation. If the SD is 0, 1/SD is taken to be the maximum weight for all other data points. The smoothing parameter is a number between 0 and 1. The value 0 corresponds to the least-squares straight line fit to the data, while the value 1 corresponds to cubic spline interpolation of the data. The function csaps also can produce a default smoothing parameter value, which for our data was $p = 0.00015$. For subsequent figures, a smoothing parameter of 0.006 (4·p where p is the csaps-derived parameter) is used because it provides a good balance between smoothing and fit to the experimental data. When comparing results for different smoothing parameter values (Fig. 2.2) we choose values that illustrate the transition from smooth approximation to interpolation.

3. Results

3.1. mR

The experimental data for mR in the normal photoperiod group gradually increase from an average of 22.8 pg/mg total RNA at day 0 to an average of 189.8 pg/mg total RNA at day 301 followed by rapid decline to basal levels near the end of the photoperiod cycle and time of spawning (Figure 3.1, (a)). The simulation results also show a gradual increase and display a shape that matches the observed data. However, at time points earlier than 200 days, the simulation results slightly overestimate the experimental data. Although the initial value for mR was chosen based on the experimental data, the simulated mR curve immediately increases to approximately 75 pg/μg total RNA. Conversely, the simulated mR peak occurs late relative to the experimental peak and underestimates the magnitude of the experimental peak. Between days 50 and 275, the simulation results are within the range of the experimental measurements.

3.2. mVg

The experimental data for mVg show low values in the first half of the cycle, which then markedly increase to a peak of 1.7×10^6pg/μg total RNA at day 301 (Figure 3.1, (b)). The simulation results again show a more gradual increase, overestimating early data points while results between days 220 and 280 match well. As in the mR simulation results, the peak is delayed relative to the experimental data and is also somewhat underestimated.

3.3. Vg_1

Unlike the upstream variables mR and mVg, the Vg_1 experimental data initially decrease (Figure 3.1, (c)). From days 50 to 225, the values remain low. Around day 250, Vg_1 levels increase slightly and plateau for about 50 days before spiking with a peak around day 325. While the peak height and final decline of the simulation results match well, the results at earlier times do not fit the experimental data well. First, the initial decline is not reflected in the simulation results. Although the initial condition of 70 mg/ml is used to match the experimental data, the simulated curve decreases too quickly. Second, the simulation results overestimate the experimental values from days 150 to 250. Lastly, the plateau preceding the spike is not reflected in the simulation results.

3.4. Ovarian uptake of Vg

In our initial simulations, we assume the ovary takes up Vg from the plasma at a constant rate. The effect of this assumption is shown in Figure 3.1, (c), dashed line. Changes to the rate of Vg uptake by the ovary CL_{1Ovg} overestimated experimental data points between 100 and 300 days for larger values, or underestimated the peak near day 325. Alternatively, it is likely that as the oocytes grow and mature, the rate of Vg uptake changes. To improve the fit of the simulations, we altered our assumption to allow a time-dependent change in Vg uptake by the ovary. We hypothesized that Vg uptake may decrease as the oocytes reach maturity late in the cycle, while other factors account for the continued increase in oocyte size (e.g. hydration). We simulated a time-dependent decrease in ovarian Vg uptake by replacing the parameter CL_{1Ovg} with a smooth approximation to a step function with a high early Vg uptake rate followed by a decrease in the Vg uptake rate at day 315. The resulting simulation better captures the small increase in experimental Vg_1 near day 250, and the large peak near day 325 (Figure 3.1).

3.5. Compressed photoperiod results

To test the response of the model to a change in input, we used the model equations and parameters developed for the normal photoperiod to simulate the response of trout to a compressed photoperiod (Figure 3.2). In this simulation, a smoothed curve derived from the experimental E2 measurements for the compressed photoperiod fish was used as input. The Vg_1 simulation output underestimates early experimental values, overestimates intermediate time points, and finally underestimates the late time points. However, because the late time points yielded very high experimental measurements that were out of the physiological range, the validity of those Vg_1 measurements is in question. While the values before about 150 days are biologically feasible, the simulation results deviate from those values, indicating that changing the E2 input curve is not enough to account for the change in Vg_1 response.

3.6. The effect of E2 input smoothing on simulation results

In the cases of all three experimentally measured variables, changing the smoothing parameter of the E2 input does not greatly change the quantitative outputs (see Figure 2.2). The simulation results using the input that is smoothed the least (64 p) also result in a less

smooth output for Vg_1, but this change is small and does not affect the fit to the experimental data.

3.7. Sensitivity to parameter changes

The response of Vg_1 simulation results to changes in most parameters is exemplified by the results obtained by changing S_{mvg} (Figure 3.3, (a)). The quantitative result scales with the parameter, but the overall shape and the relative trends over time are preserved. One exception is $k_{e,mvg}$ (Figure 3.3, (b)), which not only affects the height of the Vg_1 peak but also causes the peak to become more sharp as $k_{e,mvg}$ increases, rather than remaining rounded as in the case of S_{mvg}. It is also notable that the small early peak around day 60 is not amplified as much by a decrease in $k_{e,mvg}$ as it is by an increase in S_{mvg}. Another deviation from the typical behavior is observed in response to the parameters $k_{e,r}$, k_{on} and k_{off} (illustrated by $k_{e,r}$, Figure 3.3, (c)). While the parameter is scaled geometrically (with each parameter value being 156.25% of the next lowest value), the Vg_1 results scale linearly in response and seem to approach an upper limit.

4. Discussion

4.1. Timing of mVg peak and decline is delayed

In the current model, mVg levels stem from E2 binding to its receptor R, which forms ER and positively feeds back on mR transcription while also resulting in mVg transcription downstream. While there is an upstream positive feedback from ER to mR, this type of regulation alone is not able to capture a decrease in mVg levels that precedes the decrease in E2 levels. A negative feedback or threshold may be necessary to achieve the early peak in mVg production that is observed in the experimental data. Alternatively, the assumption that mVg is degraded at a constant rate throughout the reproductive cycle may not be appropriate. For example, there is evidence from *in vitro* studies that rising estrogen concentration can stabilize mVg levels by reducing the activity of sequence-selective mRNA endonucleases [11, 7]. Other studies with invertebrates have suggested that stabilization of mVg may be modified by interactions with other small molecules that could lead to destabilization and increase degradation [21]. Thus, an improved description might include nonlinear or seasonal changes in the degradation rate.

4.2. The addition of a time-dependent change in oocyte Vg uptake improves fit

The concentration of Vg_1 in plasma primarily reflects the balance between its rate of secretion by hepatocytes and its removal through uptake into maturing oocytes. It is also possible that some loss of Vg_1 may occur through pro-teolytic degradation or sequestration into non-ovarian tissues [31, 32]. The latter two processes are captured in the model by inclusion of a peripheral storage compartment (Vg_2) and the total body clearance parameter (CL_{Vg}), which combines all other degradative and non-degradative losses. This was considered to be the simplest description of Vg_1 kinetics that captures the essential biological processes determining its concentration. However, the sharp increase in Vg_1 levels, which does not appear in the mVg data (Figure 3.1) suggests a strong non-linear relationship or threshold effects may play a role. In preliminary simulations with the model, we attempted changing the value of parameters in the pathway between mVg and Vg_1, such

as the translational control of Vg synthesis in relationship to mVg levels by modifying the amplification factor (γ in the model). The result was unsatisfactory because it could not significantly alter the shape of the Vg_1 response (Figure 3.3, (a)).

As an alternative solution, we modified the rate of Vg uptake into oocytes to allow for rapid and constant uptake during the vitellogenic phase of oocyte growth, when the size of the individual oocytes increases the most dramatically. We then assumed that Vg uptake into oocytes decreases abruptly as they become fully mature. As can be observed in Figure 3.1 (c), the model's simulation of Vg_1 appears to be much improved by adding a change in ovarian Vg uptake rate that switches from high to low at day 315. A sudden decrease in the ovarian Vg uptake rate would cause excess Vg to rapidly accumulate in the plasma, similar to the observed data. Although further experimental studies will be necessary to establish whether the uptake rate decreases as proposed, it does appear to be biologically plausible. The uptake of Vg by oocytes is established to occur by receptor mediated endocytosis [27], which can be quite rapid in trout as demonstrated by the studies of [36, 37, 34]. Interestingly, the synthesis of the Vg uptake receptor by oocytes appears to occur early in development and during the subsequent vitellogenic growth phase of the oocytes, the Vg receptor is recycled rather than being continually synthesized [28]. Thus, in mature oocytes, the existing Vg uptake receptors could be degraded resulting in the decreased Vg uptake rate. The latter conclusion is also supported by the studies of Rodriguez et al [30] who observed a 25-fold drop in the receptor content of the trout ovary after oocyte maturation and ovulation.

4.3. Compressed photoperiod

To further test the performance of the model in predicting vitellogenesis, we collected an additional experimental data set from a group of trout that were reared under a compressed photoperiod regime. This treatment was selected because it is well established that changing day length is the primary environmental factor that regulates the reproductive cycle in trout [5]. Unnatural photoperiod regimes combining rapid increases in day length with subsequent gradual or abrupt changes to shortened day length stimulate the synthesis of hormones in the hypothalamus and pituitary that are involved in the endocrine control of reproduction [2, 6]. In our study, it was anticipated that many of the upstream variables influencing E2 synthesis and in turn, Vg synthesis would be accelerated relative to trout reared under a natural photoperiod. Thus, an important question was how well the model could predict Vg1 levels in fish reared under the compressed photoperiod. In general, the overall scale of the compressed photoperiod simulation results matches with the experimental data without parameter changes. However, the shape fits poorly. As shown in Figure 3.3, the overall shape of the results is not extremely sensitive to changes in single parameters. Thus, the difference between normal and compressed cycle Vg_1 results could not be explained by single parameter changes. Changes to either the modeled biological mechanisms or changes to multiple parameters simultaneously may account for the differences.

4.4. Conclusion

We have described a mathematical model for E2 control of Vg production in female rainbow trout. While the current model captures much of the dynamics of the experimental

data, there is room for improvement. More computationally extensive multi-parameter sensitivity analysis and optimization may reveal more complex changes to the simulation results than those found in the single parameter sensitivity analysis. Also, changing the biological mechanisms represented in the model may be necessary to better fit the experimental data. For example, future versions of the model may need to consider the role of ER-beta subtypes in modulating the regulatory control ER-alpha has on vitellogenesis. Also, an important assumption made for many of the parameters is that a constant value exists throughout the reproductive cycle. This was deemed necessary for initial development of the model, but may need to be reevaluated in the future. The physiological changes associated with ovarian development and vitellogenesis is extraordinary from the standpoint of the dramatic increases in protein synthesis by the liver and oocyte growth dynamics. Thus, it is reasonable to expect some physiological or biochemical processes characterized by a model parameter will undergo sufficient change that a constant value cannot adequately describe the rate constant of that process over the entire cycle. For example, numerical simulation results obtained using this model support the possibility that the ovarian Vg uptake rate is not constant during oocyte development. Other parameters associated with mRNA degradation such as mVg may also need to be modified to allow for seasonal changes to improve the fit to the experimental data.

The Vg model described in this study is part of a larger effort that is developing a mathematical description of the endocrine control of reproduction in female rainbow trout. The Vg model extends a submodule of a previously published model, which described the hypothalamus-pituitary-gonadal (HPG) axis in female Coho salmon (Onchorynchus kisutch) [16], by predicting plasma levels of estradiol and 17α,20β-dihydroxy-4-pregnene-3-one (DHP), as well as the gonadotropins follicle-stimulating hormone (FSH) and luteinizing hormone (LH). We plan to integrate our model of Vg production with the HPG model, which will be adapted to fit the rainbow trout experimental data collected under the normal and compressed photoperiods. Our modeling efforts complement other recent studies seeking to develop mathematical descriptions of the fish reproductive system. For example, [23] and [22] described a model for the HPG-liver axis of the Atlantic croaker (*Micropogonias undulates*), a group synchronous annual spawning estuarine fish. In their model, synthesis and secretion of Vg is described by a single rate parameter, which is stimulated by the amount of activated ER. The plasma clearance of Vg was not explicitly formulated in the model, which causes predicted Vg levels to rise to a sustained plateau. This model was then used to predict the effects of chemical exposures (a PCB mixture and cadmium) and environmental stress (prolonged hypoxia) on the HPG-liver axis [23, 22]. Another HPG-liver model was recently described for the male fathead minnow (*Pimephales promelas*), an asynchronous repeat spawning fish that is widely used in toxicological testing [39]. This model also incorporates a description of Vg similar to [23], with synthesis and secretion characterized by a single rate parameter but also includes a parameter for the first order elimination of Vg [39]. The latter model was then used to characterize the effects of exposure to two different estrogens.

The growing interest in developing mathematical models of the fish HPG-liver axis reflects the need to better understand and interpret the complex physiological changes that occur

when fish are exposed to endocrine disruptors be they chemical or associated with environmental stress (e.g. hypoxia). One area where these models are expected to be especially valuable is in future regulatory toxicity assessments. It is anticipated that in the future, greater emphasis will be placed on in vitro tests and the use of computational models to predict ecological risk [1]. Mathematical models that incorporate parameters that can be measured by in vitro methods (e.g. mVg, mR) and subsequently linked to tissue and organism level changes such as ovarian development and spawning are particularly needed [38, 17]. Our present Vg model moves towards this goal by providing a more detailed description of vitellogenesis by including parameters for gene expression of the estrogen receptor and Vg along with a more physiologically accurate description of Vg clearance. Including descriptions of the dynamics of gene expression is important, as it demonstrates the potential for more widespread characterization of time-course gene expression data collected with DNA microarrays and other high-throughput methods. The full potential of incorporating gene expression data into whole animal kinetic models was elegantly demonstrated for the corticosteroid, methylprednisolone, in the rodent liver by Jin et al [13]. We have recently used time-course microarray analysis to characterize gene expression changes in the pituitary, ovary and liver of female trout during the reproductive cycle [20]. Thus, an important goal for our modeling effort is to incorporate the results from gene expression studies into our model, to eventually include pathways not yet represented in the HPG or Vg models.

Also, in general, the trout is a good example of a seasonally breeding fish with group synchronous ovarian development. We propose that other species of fish with this type of ovarian development could be analyzed similarly.

Acknowledgments

We thank the National Science Foundation for support under grant DMS-054069377. Kaitlin Sundling was supported by National Institutes of Health training grant T32GM08349 (Biotechnology Training Program) and the University of Wisconsin Medical Scientist Training Program.

References

1. Ankley GT, Bennett RS, Erickson RJ, Hoff DJ, Hornung MW, Johnson RD, Mount DR, Nichols JW, Russom CL, Schmieder PK, Serrrano JA, Tietge JE, Villeneuve DL. Adverse outcome pathways: A conceptual framework to support ecotoxicology research and risk assessment. Environmental Toxicology and Chemistry. 2010; 29:730–741. URL http://dx.doi.org/10.1002/etc.34. [PubMed: 20821501]
2. Bon E, Breton B, Govoroun M, Le Menn F. Effects of accelerated photoperiod regimes on the reproductive cycle of the female rainbow trout: II Seasonal variations of plasma gonadotropins (GTH I and GTH II) levels correlated with ovarian follicle growth and egg size. Fish Physiology and Biochemistry. 1999; 20:143–154.
3. Boyce-Derricott J, Nagler JJ, Cloud JG. Variation among rainbow trout (On-corhynchus mykiss) estrogen receptor isoform 3′ untranslated regions and the effect of 17 β-estradiol on mRNA stability in hepatocyte culture. DNA and cell biology. 2010; 29:229–234. [PubMed: 20438355]
4. Bromage, N.; Randall, C.; Davies, B.; Thrush, M.; Duston, J.; Carillo, M.; Zanuy, S. Photoperiodism and the control of reproduction and development in farmed fish. In: Lahlou, B.; Vitiello, P., editors. Aquaculture: Fundamental and Applied Research. Am. Geophys. Union; Washington, D.C.: 1993. p. 81-102.

5. Bromage N, Porter M, Randall C. The environmental regulation of maturation in farmed finfish with special reference to the role of photoperiod and melatonin. Aquaculture. 2001; 197:63–98. URL http://www.sciencedirect.com/science/article/B6T4D-4313NM4-5/2/c982e2d89b0011c0dc686831087f3b14.

6. Choi S, Lee CH, Park W, Kim DJ, Sohn YC. Effects of shortened photoperiod on gonadotropin-releasing hormone, gonadotropin, and vitellogenin gene expression associated with ovarian maturation in rainbow trout. Zoological Science (Tokyo). 2010; 27:24–32.

7. Cunningham KS, Dodson RE, Nagel MA, Shapiro DJ, Schoenberg DR. Vigilin binding selectively inhibits cleavage of the vitellogenin mRNA 3′-untranslated region by the mRNA endonuclease polysomal ribonuclease 1. Proceedings of the National Academy of Sciences of the United States of America. 97

8. Davies B, Bromage N, Swanson P. The brain-pituitary axis of female rainbow trout Oncorhynchus mykiss: Effects of photoperiod manipulation. General and Comparative Endocrinology. 1999; 115:155–166. [PubMed: 10375474]

9. Duston J, Bromage NR. Photoperiodic mechanisms and rhythms of reproduction in the female rainbow trout. Fish Physiology and Biochemistry. 1986; 2:35–51. [PubMed: 24233166]

10. Duston J, Bromage NR. The entrainment and gating of the endogenous circannual rhythm of reproduction in the female rainbow trout (Salmo gairdneri). Journal of Comparative Physiology A. 1988; 164:259–268.

11. Flouriot G, Pakdel F, Valotaire Y. Transcriptional and post-transcriptional regulation of rainbow trout estrogen receptor and vitellogenin gene expression. Molecular and cellular endocrinology. 1996; 124:173–183. [PubMed: 9027336]

12. Hook, S.; Nagler, J.; Cavileer, T.; Verducci, J.; Liu, Y.; Sundling, K.; Hayton, W.; Kim, J.; Schultz, I. Gene expression profiles in the pituitary, ovary, and liver of female rainbow trout during the reproductive cycle. submitted

13. Jin JY, Almon RR, DuBois DC, Jusko WJ. Modeling of corticosteroid pharmacogenomics in rat liver using gene microarrays. Journal of Pharmacology and Experimental Therapeutics. 2003; 307:93–109. [PubMed: 12808002]

14. Jusko WJ, Ko HC. Physiologic indirect response models characterize diverse types of pharmacodynamic effects. Clinical pharmacology and therapeutics. 1994; 56:406–419. [PubMed: 7955802]

15. Kim, J. Doctoral Thesis. Ohio State University; 2004. Pharmacokinetics and Pharmacodynamics of Protein Turnover and Production in Vivo.

16. Kim J, Hayton WL, Schultz IR. Modeling the brain-pituitary-gonad axis in salmon. Marine environmental research. 2006; 62:S426–S432. [PubMed: 16716390]

17. Kramer VJ, Etterson MA, Hecker M, Murphy CA, Roesijadi G, Spade DJ, Spromberg JA, Wang M, Ankley GT. Adverse outcome pathways and ecological risk assessment: Bridging to population-level effects. Environmental Toxicology and Chemistry. 2011; 30:64–76. [PubMed: 20963853]

18. Katsu Y, Lange A, Miyagawa S, Urushitani H, Tatarazako N, Kawashima Y, Tyler CR, Iguchi T. Cloning, expression and functional characterization of carp (Cyprinus carpio) estrogen receptors and their differential activations by estrogens. Journal of Applied Toxicology. 2013; 33:41–49. [PubMed: 21721020]

19. Leanos-Castaneda O, Van Der Kraak G. Functional characterization of estrogen receptor, ERa and ERb, mediating vitellogenin production in the liver of rainbow trout. Toxicology and Applied Pharmacology. 2007; 224:116–125. [PubMed: 17662327]

20. Liu Y, Verducci J, Schultz I, Hook S, Nagler J, Craciun G, Sundling K, Hayton W. Time course analysis of microarray data for the pathway of reproductive development in female rainbow trout. Stat Anal Data Min. 2009; 2:192–208.

21. Mao C, Flavin KG, Wang S, Dodson R, Ross J, Shapiro DJ. Analysis of RNA-protein interactions by a microplate-based fluorescence anisotropy assay. Analytical Biochemistry. 2006; 350:222–232. [PubMed: 16448619]

22. Murphy CA, Rose KA, Rahman MS, Thomas P. Testing and applying a fish vitellogenesis model to evaluate laboratory and field biomarkers of endocrine disruption in atlantic croaker

(micropogonias undulatus) exposed to hypoxia. Environmental Toxicology and Chemistry. 2009; 28:1288–1303. [PubMed: 19642826]

23. Murphy CA, Rose KA, Thomas P. Modeling vitellogenesis in female fish exposed to environmental stressors: Predicting the effects of endocrine disturbance due to exposure to a PCB mixture and cadmium. Reproductive Toxicology. 2005; 19:395–409. [PubMed: 15686873]
24. Nagler JJ, Cavileer T, Sullivan J, Cyr DG, R C III. The complete nuclear estrogen receptor family in the rainbow trout: Discovery of the novel ER α2 and both ER β isoforms. Gene (Amsterdam). 2007; 392:164–173. [PubMed: 17307310]
25. Nagler JJ, Davis TL, Modi N, Vijayan MM, Schultz I. Intracellular, not membrane, estrogen receptors control vitellogenin synthesis in the rainbow trout. General and comparative endocrinology. 2010; 167:326–330. [PubMed: 20346361]
26. Nelson ER, Habibi HR. Functional significance of nuclear estrogen receptor subtypes in the liver of goldfish. Endocrinology. 2010; 151:1668–1676. [PubMed: 20194729]
27. Opresko LK, Wiley HS. Receptor-mediated endocytosis in Xenopus oocytes. I. Char-acterization of the vitellogenin receptor system. Journal of Biological Chemistry. 1987; 262:4109–4115. [PubMed: 3031062]
28. Perazzolo LM, Coward K, Davail B, Normand E, Tyler CR, Pakdel F, Schneider WJ, Menn FL. Expression and localization of messenger ribonucleic acid for the vitellogenin receptor in ovarian follicles throughout oogenesis in the rainbow trout, Oncorhynchus mykiss. Biology of reproduction. 1999; 60:1057–1068. [PubMed: 10208965]
29. Piferrer F, Donaldson EM. Uptake and clearance of exogenous estradiol-17 beta and testosterone during the early development of coho salmon (Oncorhynchus kisutch), including eggs, alevins and fry. Fish Physiology and Biochemistry. 1994; 13:219–232. [PubMed: 24198192]
30. Rodriguez JN, Bon E, Menn FL. Vitellogenin receptors during vitellogenesis in the rainbow trout Oncorhynchus mykiss. The Journal of experimental zoology. 1996; 274:163–170. [PubMed: 8882494]
31. Schultz IR, Orner G, Merdink JL, Skillman A. Dose-response relationships and pharmacokinetics of vitellogenin in rainbow trout after intravascular administration of 17[alpha]-ethynylestradiol. Aquatic Toxicology. 2001; 51:305–318. [PubMed: 11090892]
32. Skillman AD, Nagler JJ, Hook SE, Small JA, Schultz IR. Dynamics of 17α-ethynylestradiol exposure in rainbow trout (oncorhynchus mykiss): absorption, tissue distribution, and hepatic gene expression pattern. Environmental toxicology and chemistry / SETAC. 2006; 25:2997–3005. [PubMed: 17089724]
33. Taylor CM, Blanchard B, Zava DT. A Simple Method to Determine Whole Cell Uptake of Radiolabeled Estrogen and Progesterone and Their Subcellular-Localization in Breast-Cancer Cell-Lines in Monolayer-Culture. Journal of Steroid Biochemistry and Molecular Biology. 1984; 20:1083–1088.
34. Tyler C, Sumpter J, Handford R. The dynamics of vitellogenin sequestration into vitellogenic ovarian follicles of the rainbow trout, salmo gairdneri. Fish Physiology and Biochemistry. 1990; 8:211–219. [PubMed: 24221984]
35. Tyler CR, Sumpter JP. Oocyte growth and development in teleosts. Reviews in Fish Biology and Fisheries. 1996; 6:287–318.
36. Tyler CR, Sumpter JP, Bromage NR. In vivo ovarian uptake and processing of vitellogenin in the rainbow trout, salmo gairdneri. Journal of Experimental Zoology. 1988; 246:171–179. URL http://dx.doi.org/10.1002/jez.1402460209.
37. Tyler CR, Sumpter JP, Bromage NR. Selectivity of protein sequestration by vitellogenic oocytes of the rainbow trout, salmo gairdneri. Journal of Experimental Zoology. 1988; 248:199–206. URL http://dx.doi.org/10.1002/jez.1402480211.
38. Watanabe KH, Andersen ME, Basu N, Carvan MJ, Crofton KM, King KA, Suñol C, Tiffany-Castiglioni E, Schultz IR. Defining and modeling known adverse outcome pathways: Domoic acid and neuronal signaling as a case study. Environmental Toxicology and Chemistry. 2011; 30:9–21. [PubMed: 20963854]
39. Watanabe KH, Li Z, Kroll KJ, Villeneuve DL, Garcia-Reyero N, Orlando EF, Sepúlveda MS, Collette TW, Ekman DR, Ankley GT, Denslow ND. A computational model of the hypothalamic-

pituitary-gonadal axis in male fathead minnows exposed to 17α-ethinylestradiol and 17β-estradiol. Toxicological Sciences. 2009

40. Zohar Y, Munoz-Cueto JA, Elizur A, Kah O. Neuroendocrinology of reproduction in teleost fish. General and Comparative Endocrinology. 2010; 165:438–455. [PubMed: 19393655]

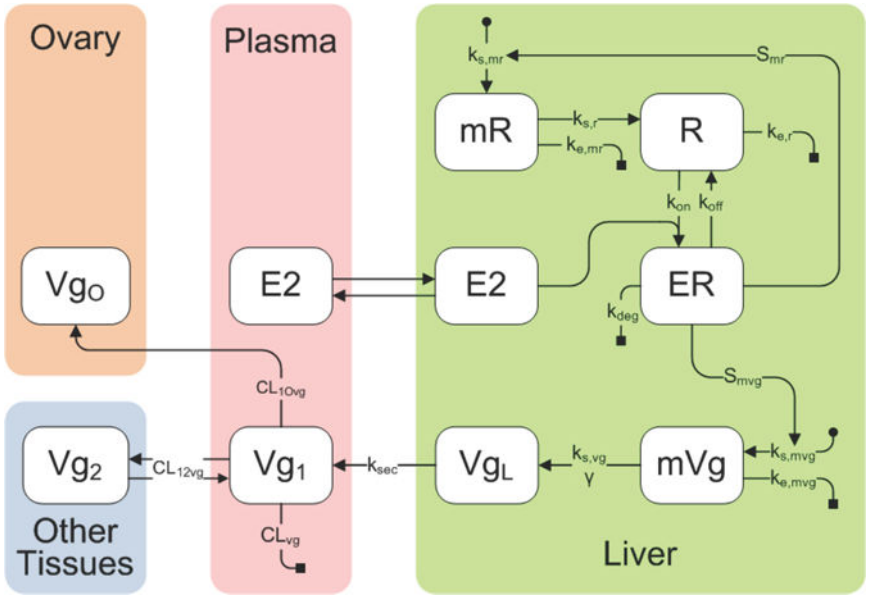

FIGURE 2.1.

Schematic diagram of the model describing Vg dynamics in female rainbow trout. The model contains compartments for the liver, plasma, ovary and remaining peripheral tissues and the associated pharmacokinetic variables and parameters that predict Vg synthesis. Variables are defined in section 2.1 on the previous page and parameters are defined in Table 1.

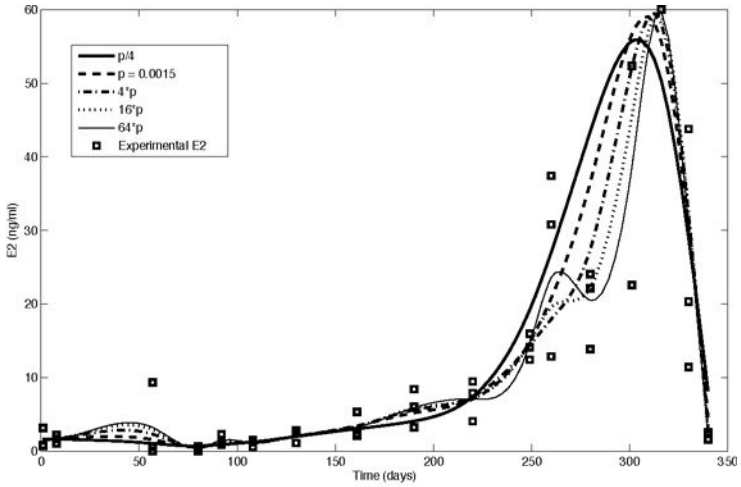

(A)

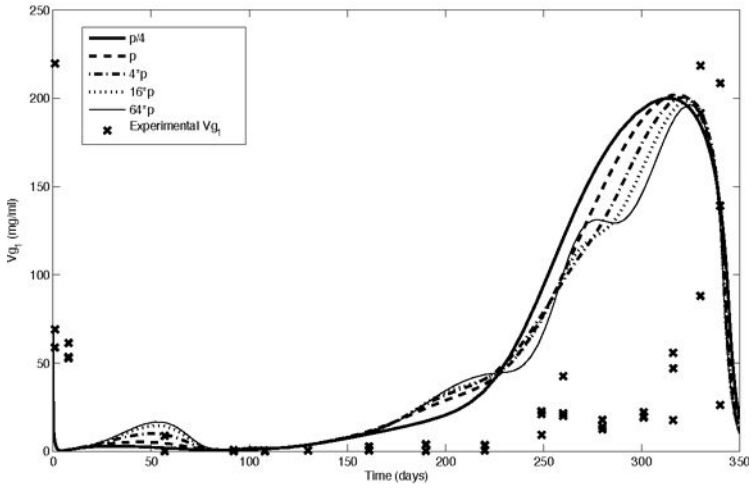

(B)

FIGURE 2.2.

The effect of varying the amount of smoothing on the model input and simulation results in trout reared under a normal photoperiod cycle. The numbers in the figure legends represent different values of the smoothing parameter used by the MATLAB function csaps (larger numbers correspond to less smoothing, but better interpolation). (a) The experimentally observed concentration of E2 in plasma and smoothed model input, (b) The observed concentration of Vg in plasma (Vg_1) and simulation results.

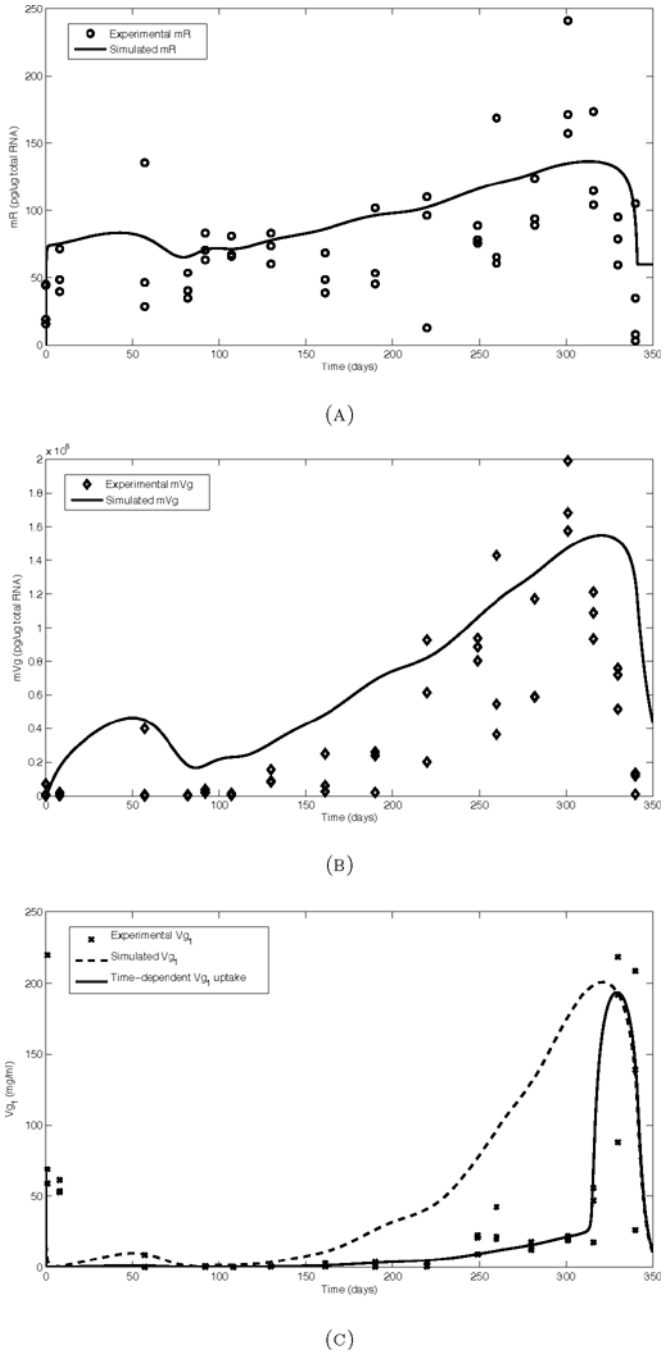

FIGURE 3.1.

Model simulations (solid and dashed lines) and observed data from trout reared under a normal photoperiod cycle. All simulations were performed using the smoothing parameter 4·p for the E2 input. (a) mR (estrogen receptor mRNA), (b) mVg (Vg mRNA), (c) Vg_1 (Vg in plasma).

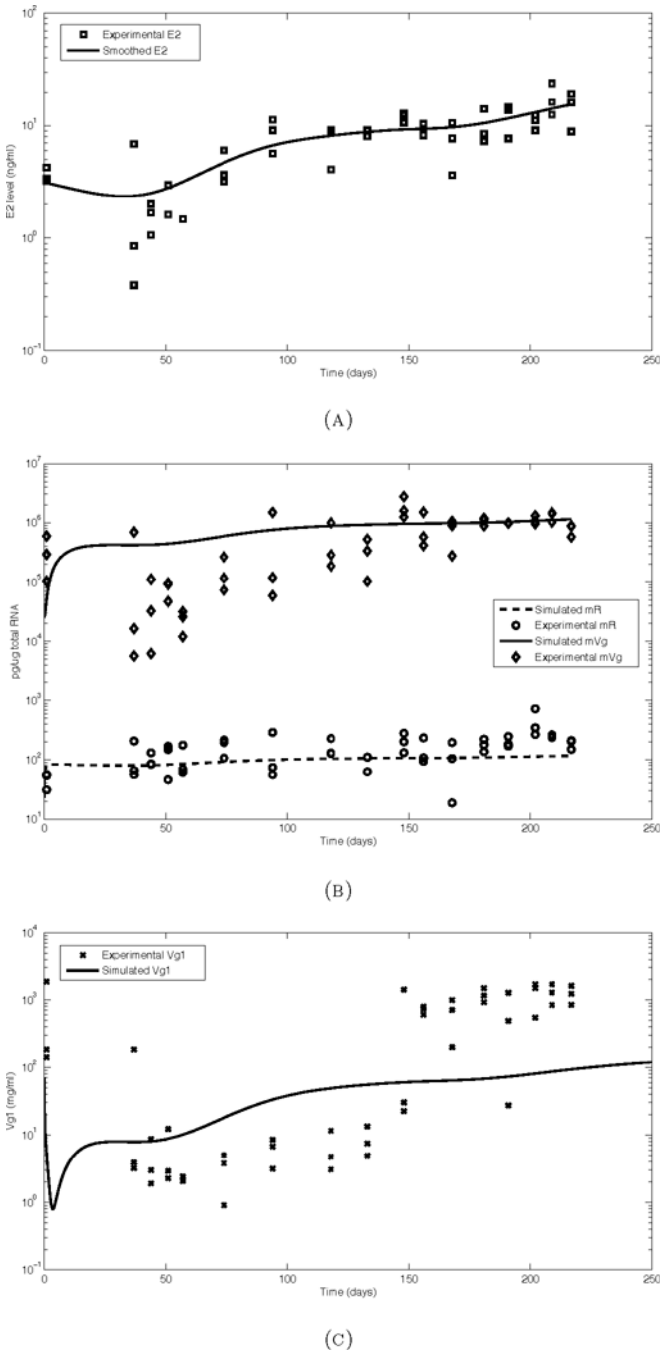

FIGURE 3.2.

Model simulations (solid lines) and observed data from trout reared under a compressed photoperiod cycle. All simulations were performed using the smoothing parameter 4·p for the E2 input. (a) E2, (b) mR and mVg, (c) Vg_1. Note use of logarithmic scale on Y-axis.

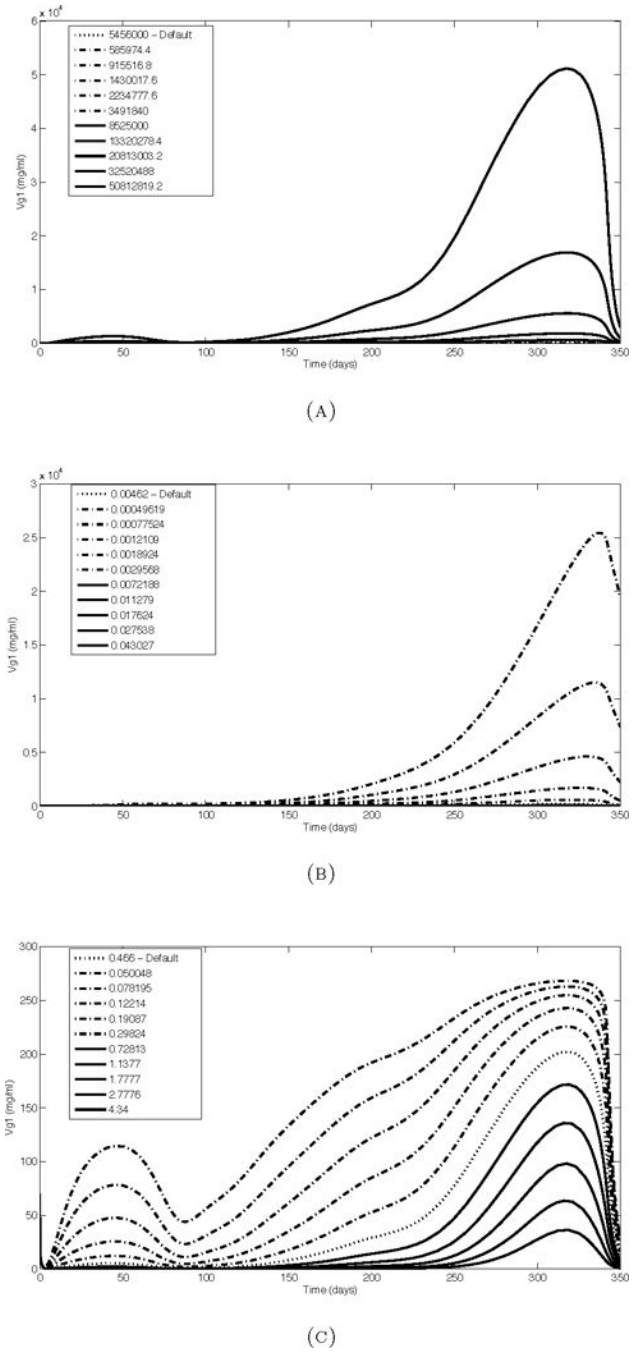

FIGURE 3.3.

Example Vg_1 simulation results after scaling model parameters one at a time. (a) S_{mvg} shows the most common response to parameter changes. (b) Altering $k_{e,\,mvg}$ results in a sharper peak. (c) Scaling k_{er} (shown), k_{on} and k_{off} results in a more linear response.

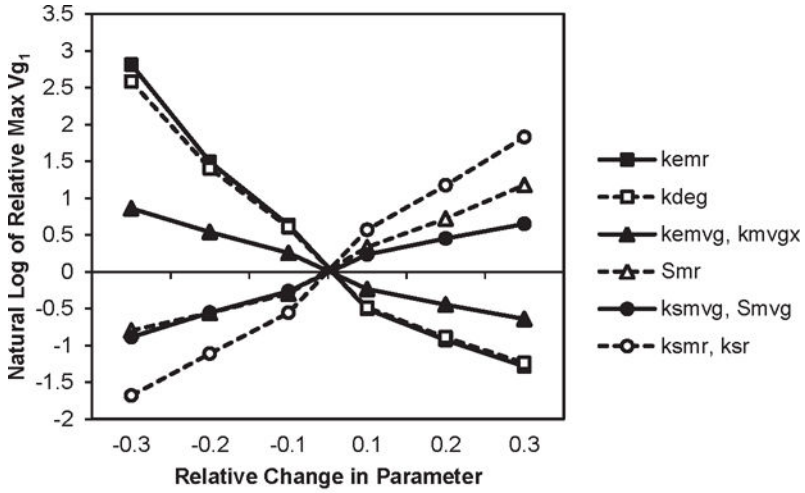

(A)

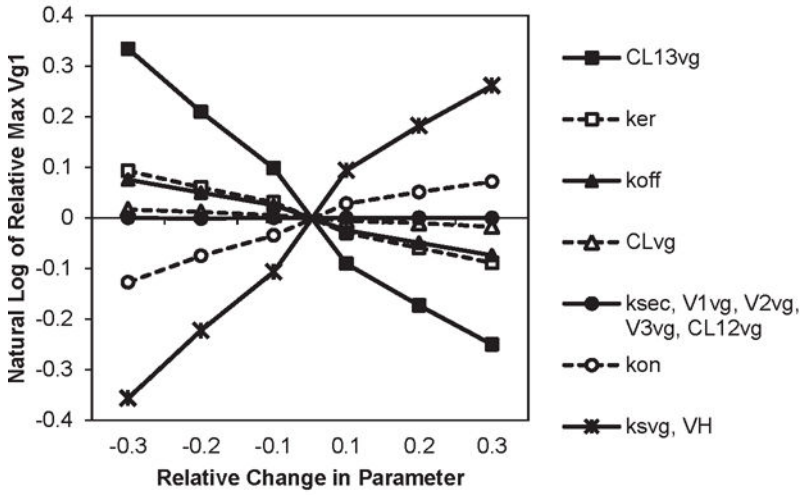

(B)

FIGURE 3.4.

Relative change in maximum Vg_1 values obtained by changing model parameter values by ±10%, ±20%, and ±30%. Part (a) shows results for parameters that have the most effect of maximum Vg_1, and part (b) shows results for the remaining parameters (note that the Y-axes of the two plots have different scales).

TABLE 1

Parameters and initial conditions used for mathematical modeling.

Param.	Explanation	Value	Units
$k_{s,mr}$	Rate of mR synthesis	30	pg/μg RNA/hr
$k_{e,mr}$	Rate constant for mR degradation	5	hr^{-1}
S_{mr}	Maximal stimulatory fold-increase in mR synthesis	0.0667	g liver/fmol
$k_{s,r}$	Rate constant for R synthesis	0.00113	$(pg/\mu g\ RNA)^{-1}$ fmol/g liver/hr
$k_{e,r}$	Rate constant for R degradation	0.0466	hr^{-1}
k_{on}	Association rate constant for ER	0.826	$(ng/g\ liver)^{-1}\ hr^{-1}$
k_{off}	Dissociation rate constant for ER	0.347	hr^{-1}
k_{deg}	Rate constant for degradation of ER complex	0.0766	hr^{-1}
$k_{s,mvg}$	Rate of mVg synthesis	$6.93 \cdot 10^{-5}$	pg/μg RNA/hr
$k_{e,mvg}$	Rate constant for mVg degradation	0.0046	hr^{-1}
k_{mvg}	Scaling factor for mVg concentration	1000	pg/μg RNA
S_{mvg}	Stimulatory fold-increase in Vg synthesis	$5.456 \cdot 10^{6}$	g liver/fmol
$k_{s,vg}$	Rate constant for Vg synthesis	$9.0213 \cdot 10^{-5}$	fmol/g liver/hr
k_{sec}	Rate constant for Vg secretion	7.87	hr^{-1}
γ	Amplification factor on the translation of Vg	2.48	unitless
V_H	Liver weight	15	g/kg
CL_{vg}	Total body clearance of Vg	29.3	ml/hr/kg
CL_{12vg}	Intercompartmental clearance between central and peripheral	42.2	ml/hr/kg
CL_{1Ovg}	Intercompartmental clearance from plasma to ovary	515	ml/hr/kg
V_{1vg}	Volume of distribution of Vg in plasma	240	ml/kg
V_{2vg}	Volume of distribution of Vg in peripheral tissues	318	ml/kg
$mR(0)$	Initial concentration of estrogen receptor mRNA	22.8	pg/μg total RNA
$R(0)$	Initial concentration of estrogen receptor protein	0.1	fmol/g liver
$ER(0)$	Initial concentration of estrogen-estrogen receptor complex	0.1	fmol/g liver
$mVg(0)$	Initial concentration of Vg mRNA	$2.5989 \cdot 10^{4}$	pg/μg total RNA
$Vg_L(0)$	Initial concentration of Vg in liver	0.1	fmol/g liver
$Vg_1(0)$	Initial plasma concentration of Vg	70	mg/ml
$Vg_2(0)$	Initial concentration of Vg in peripheral tissues	0.009	mg/ml
$Vg_O(0)$	Initial concentration of Vg in ovary	0	fmol/g ovary